Supporting Information

Xi et al. 10.1073/pnas.1712195114

SI Materials and Methods

Fabrication.

To fabricate PDMS microtubes, a metal wire (typically made of copper or tungsten) was vertically immersed into a freshly mixed PDMS (mixture of Sylgard 184 silicone elastomer base and Sylgard 184 silicone elastomer curing agent, 10:1 by weight) pool, as depicted in Fig. S1. The metal wire was then electrically heated up to ~100 °C. This generated a heat field close to the metal wire that initiated PDMS curing. A thin layer of cured PDMS formed around the wire and its thickness depended on the period of heating. When the metal wire was drawn out vertically above the liquid level, a second thin layer of viscous uncured PDMS was formed around the wire, which was further cured by hot air at ~95 °C in a cylindrical heating unit (Fig. S1). This generates a PDMS microtube enclosing the metal wire at the central axis. To produce a soft hollow tube, the metal wire was peeled off during a sonication process in acetone solution which washed off unreacted elastomer curing agent and caused slight swelling in the polymer, thereby loosening the PDMS-metal contact. The detached PDMS microtubes were then baked in an oven to remove any acetone remnant and stored for future use.

To fabricate microtubes from UV-curable polymer, a metal wire was pulled out of a pre-cured polymer (Mypolymer, MY-134-XP8, My Polymers Ltd.) pool into a glass chamber. Instead of electrical heating, the thin viscous polymer layer coated around the metal wire was cured on-site

under a UV mercury lamp. The peeling off procedure was done using a similar method as mentioned above. All the assembly work to fabricate microfluidic chips using PDMS microtubes was performed manually, guided with frameworks made by 3D printing or laser cutting.

Surface analyses.

For SEM imaging, the metal wires were fixed on a metal stage using double sided adhesive carbon tapes. The wires were observed using a JEOL scanning electron microscope (JSM-6010LV) with a 7 keV acceleration voltage. For the AFM analyses, the microtubes were cut into two halves from the midplane to expose the inner surfaces. The opened microtubes were then placed on a glass slide with the inner surface facing upward. The surface topography was characterized under ambient conditions by tapping mode AFM (JPK Instruments AG, Germany) at a scan rate of 0.5 Hz and images were acquired as 512 × 512 lines. The surface roughness analyses were subsequently extracted from the arithmetic average roughness (Ra), the root-mean-squared roughness (Rq) and the peak-to-valley height (Rm) measurements by evaluating the obtained AFM images.

Valving and actuation set-ups.

To make the valve, a PDMS microtube with an ID of 100 μm was mounted inside a laser-cut straight groove and a pincher was placed underneath to compress the microtube against a flat surface. The head of the pincher, which pinched the tube, has a width of 1mm. The pincher was then connected to a solenoid, which has an extension range of 2 mm and was controlled by a relay that was controlled by a digital signal generator. The solenoid responded to the digital signal to pinch (+5V) onto or release (0V) from the microtube with a maximum frequency of up to ~75 Hz.

The open and close states of the microtube were monitored by measuring the fluorescent intensity due to the aqueous fluorescein solution flowing in the microtube. The videos of valving behavior were recorded using an Olympus IX71 microscope with a high speed camera (Phantom v9, Vision Research Inc., USA) at a rate of 1000 images/second.

The peristaltic pump was installed with first mounting a PDMS microtube with ID = 100 μm as a pump tube onto a peristaltic pump (model P720, Instech Laboratories, Inc.) according to the P720 manual. The peristaltic pump was operated between 0.4 – 14 rpm and the motion of a column of water in the outlet tubing (0.5 mm ID) was used to calculate the pumping rate.

The formation of microchannels of arbitrary shapes.

The templates of circular, triangular, square, pentagonal, planar spiral, cylindrical and serpentine shapes that were used as guides to form different microtube patterns were fabricated either by 3D printing or laser cutting methods. The 2D and 3D channels were fabricated by bending or winding the PDMS microtubes into these templates.

Cell culture and seeding.

Madin-Darby Canine Kidney (MDCK) stable cell line expressing H1-GFP and HeLa cells were used. The cells were cultured in full Dulbecco's Modified Eagle Medium (DMEM, Sigma-Aldrich) supplemented with 1% antibiotics (penicillin/streptomycin, Invitrogen) and 10% Fetal Bovine Serum (FBS, Sigma-Aldrich) at 37 ºC in a humidified atmosphere containing 5% CO_2. Human Umbilical Vein Endothelial Cells (HUVECs) were cultured in M-199 Medium (Sigma-Aldrich) supplemented with 20% FBS, 2 mmol/L penicillin/streptomycin, 2 mmol/L amphotericin

B, 2mmol/L L-glutamine, 10 mmol/L HEPES, 30-50 μg/ml endothelial cell growth supplement (Corning) and 100 μg/ml heparin sodium salt.

The cells were trypsinized and harvested at 70% confluence from culture flasks and re-suspended in the growth medium before seeding in the microtubes. Cell seeding into PDMS microtubes was performed by directly injecting a solution of 1×10^6 cells mL^{-3} into the microtubes, followed by culturing for 30 – 60 minutes to allow cell attachment on the inner walls of the microtubes. This seeding procedure was repeated once after 180º rotation of the microtubes, which were subsequently submerged into full media for long-term culture. After 48 hours, cells were fixed using 4% paraformaldehyde for further imaging. For endothelial cells, the endothelialized PDMS microtubes were connected to a home-made microfluidic system and perfused with the growth medium at a flow rate of 50 μL/min for 48 hours before fixation. The fixed HUVECs in microtubes were stained with DAPI for confocal imaging. A Nikon confocal microscope equipped with a 20× objective was used to examine the cells in the microtubes. A z-stack of the entire tubular cell sheets was obtained at 1 μm per step. ImageJ (NIH) was then used to reconstruct the 3D tubular structure formed during epithelialization or endothelialization of the microtubes.

Microfluidics and image analysis.

Microfluidic assemblies formed from the microtubes were put together manually using 3D-printed supporting frames. The microtubes were connected to epoxy sealed blunt end tips (Fisnar Inc.) and solutions containing cells, blood or microparticles were routed into the microtubes using a syringe pump (NE-1000, New Era Pump Systems Inc., USA). To connect the microtube to an expanded outlet, a pulled glass capillary coated with a silane anti-adhesion layer was first inserted into the

microtube. The junction was later sealed by PDMS molding and the formation of the expanded channels in the outlet was obtained by pulling out the inserted glass capillary. Videos and images showing the flow at the outlet of the microtube-based devices were captured using an inverted epifluorescence microscope (Olympus IX71) equipped with a high speed camera (Phantom v9, Vision Research Inc., USA). The acquired high speed videos were then analysed using ImageJ (NIH) and Imaris 8.3.1 (bitplane) software to track individual micro-entities and calculate the focus efficiency, lateral distribution of microparticles and separation performance.

Designs of microchannels.

Microfluidic channels for focusing of microparticles were designed to enable inertial focusing behaviour. The effect of inertial focusing is closely relevant to the ratio between the particle diameter (a), the hydraulic diameter (D_h) (defined as the diameter in case of circular channels), the channel curvature and flow rate. The microtubes with a circular diameter of 100 μm were selected, as particles with sizes similar to that of cells (7 – 25 μm in diameter) were all above the stated a/D_h threshold of 0.07.

Physical adsorption of catalase into PDMS microtubes and optical imaging of locomotion.

A PDMS microtube with ID = 100 μm was injected with 100 μL of catalase solution (2 mg/mL) and incubated at 37 ºC overnight. The tube was cut into pieces of submillimeter in length and rinsed briefly with 1X PBS. These pieces were then placed into different hydrogen peroxide solution and imaged under an optical microscope. Videos of the locomotion were acquired by a high-speed camera (Photonic Science Limited) at 50 frames/s.

Triboelectric measurements.

A PDMS microtube with an ID = 100 μm and OD = 150 μm was used as a triboelectric sensor. A portion (~ 3 – 5 mm) at the middle of the microtube was coated with a layer of 20 nm Platinum by sputtering. This layer was later connected to a piece of tinfoil for better current conduction. A syringe pump was used to control the KCl solution movement inside the microtube and a programmable electrometer (Keithley 6517B) was adopted to detect the output current signal of the sensor.

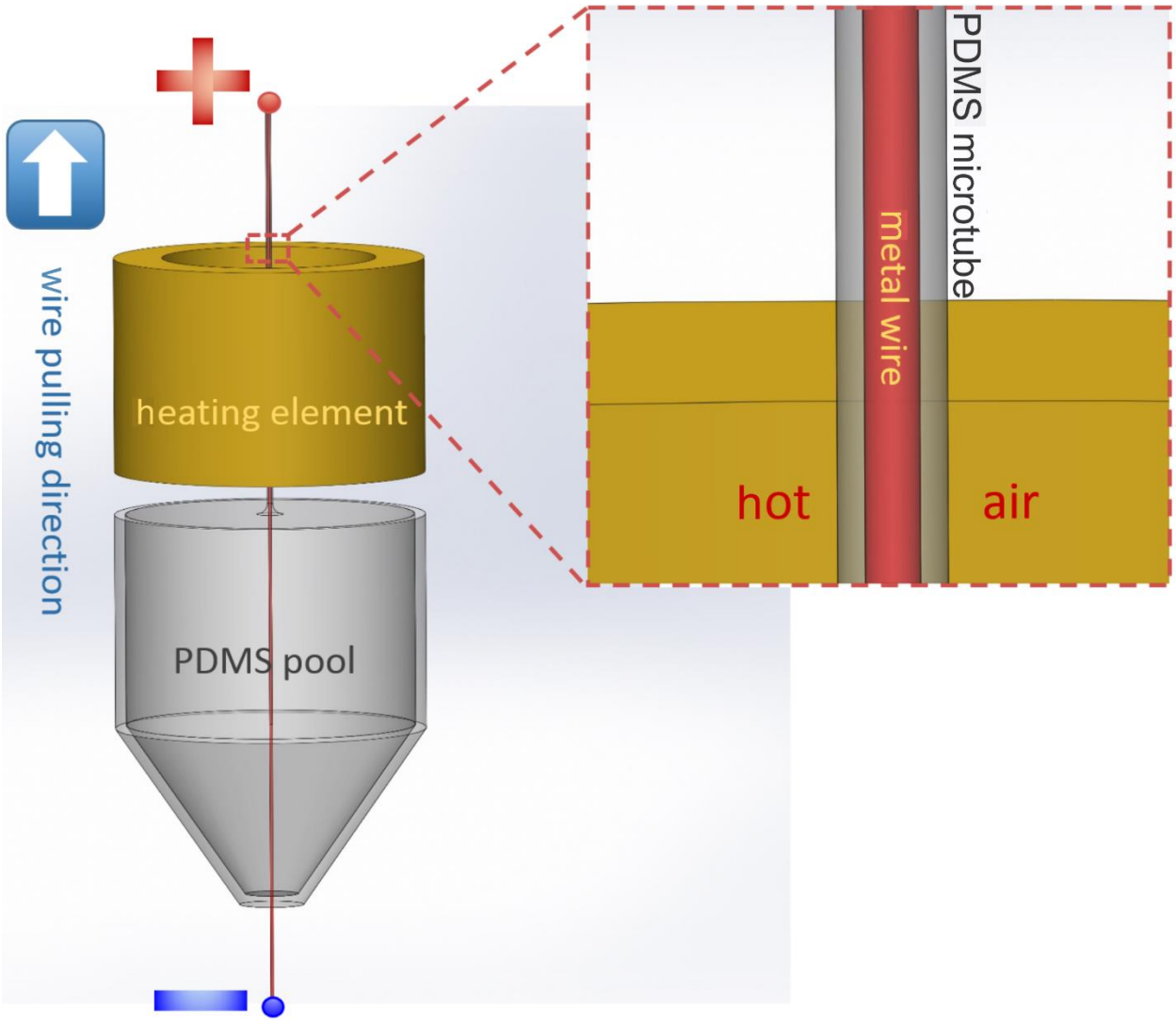

Fig. S1. Schematic view of the experimental set-up for fabrication of PDMS microtubes.

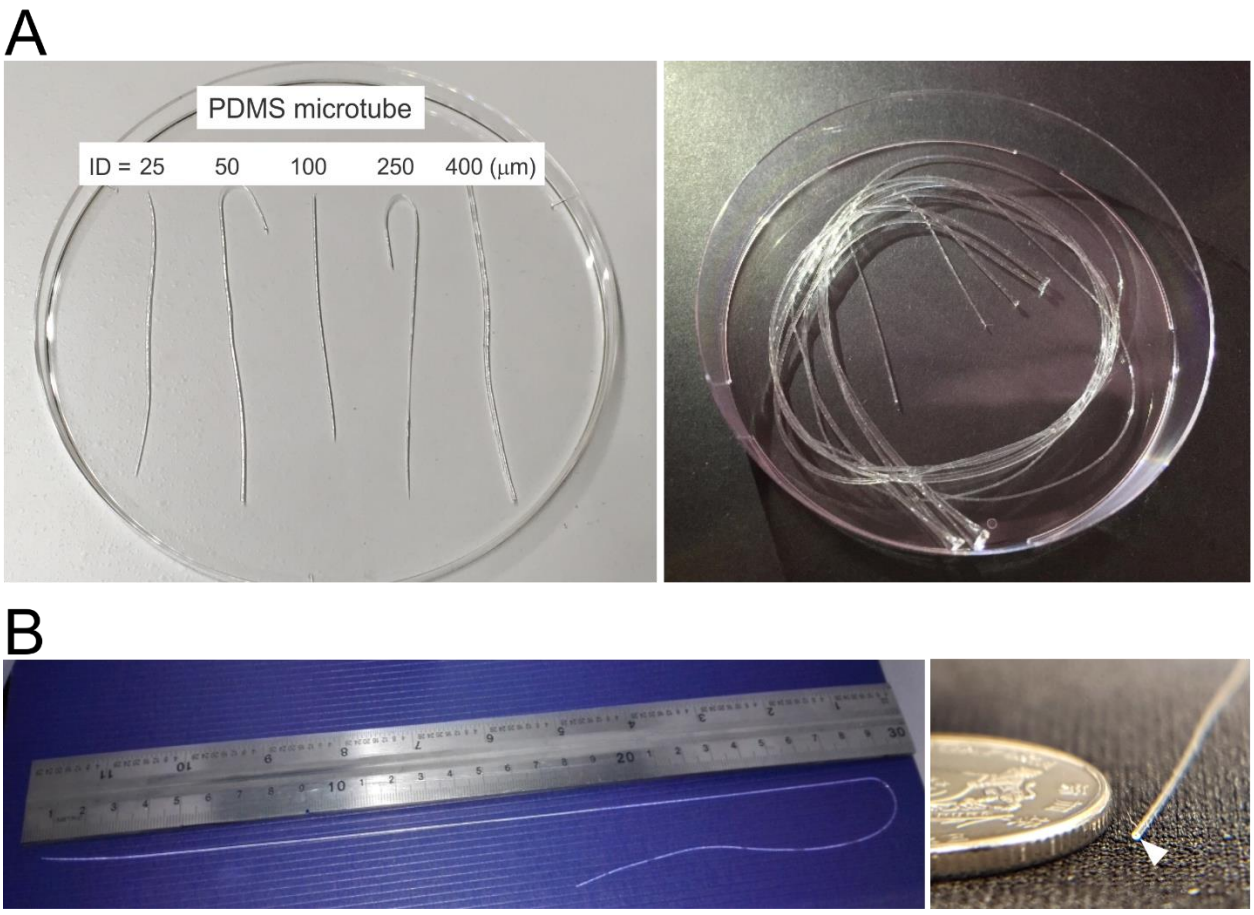

Fig. S2. Photos of (*A*) PDMS microtubes with different inner diameters (ID) and (*B*) left, a 45 cm long PDMS microtube with ID = 50 μm and right, the opening of the microtube (white arrow).

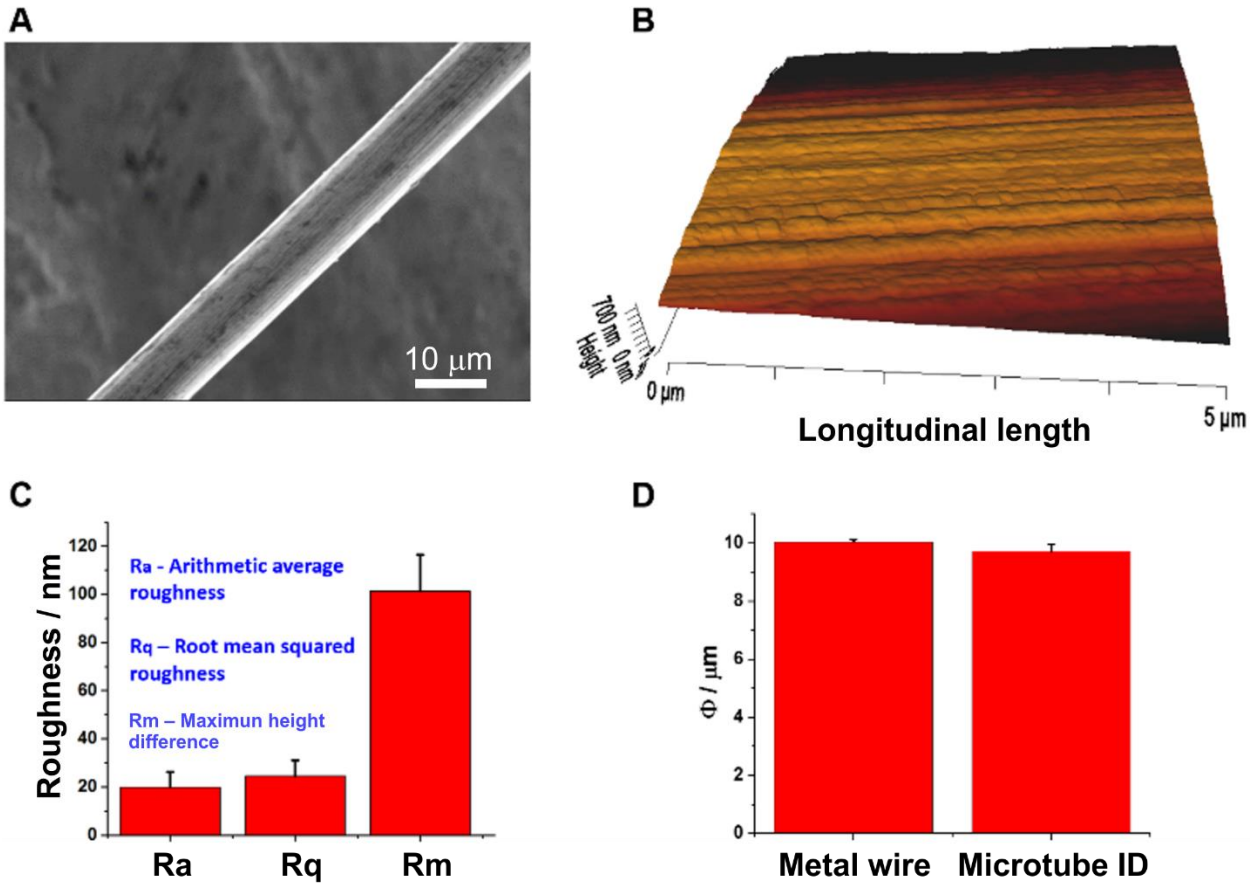

Fig. S3. (*A*) A SEM image showing a tungsten wire with diameter of 10 µm. (*B*) AFM topography showing the inner surface of a PDMS microtube (ID = 10 µm). (*C*) AFM roughness analysis of the inner surface of the microtube presented in (*B*). (*D*) The metal wire diameter and the ID of the PDMS microtube manufactured from the wire.

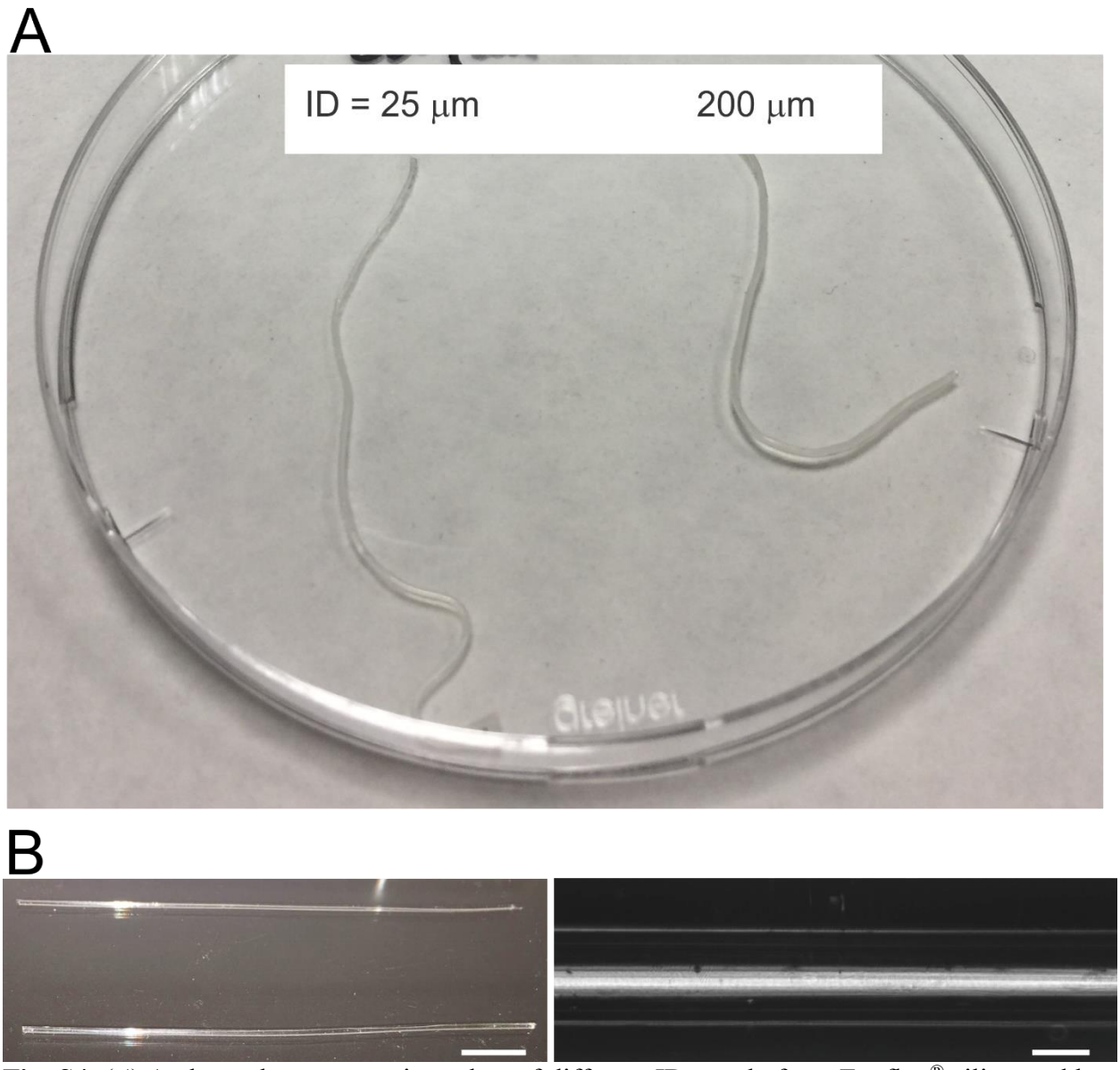

Fig. S4. (*A*) A photo shows two microtubes of different IDs made from Ecoflex® silicon rubber. (*B*) Two microtubes made from UV-curable polymer (left) and the optical image (right) showing the ID (250 μm) of the microtube. Scale bar: 5mm (left) and 150μm (right).

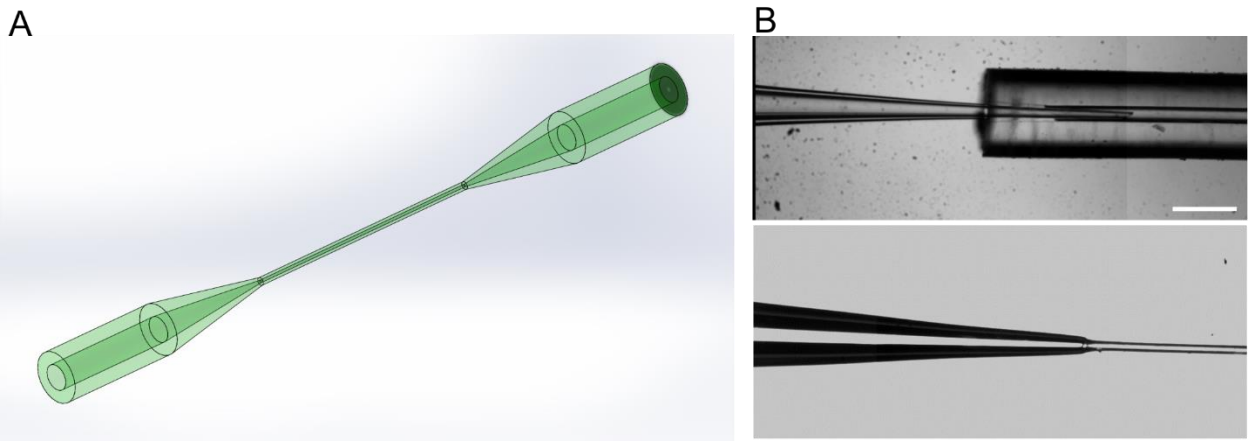

Fig. S5. (*A*) Schematic illustration showing a PDMS microtube with two expanded openings. (*B*) optical images showing top, inserted glass capillary as a template for opening expansion for a microtube of inner diameters (ID) = 25 μm, and bottom, the expanded opening that is compatible with commercially available blunt needles. Scale bar, 100 μm.

Table S1. The mechanical properties of the PDMS microtubes compared with commercially available silicone tubing.

Property	**PTFE tubing**	**SEBS tubing**	**Our microtube**
Minimum inner diameter (μm)	500	360	10
Tensile strength (MPa)	21 – 35	10	3 – 7
Elongation at break (%)	200 – 400	800 – 1000	200 – 400
Hardness (Shore)	D: 50 – 65	A:65	A: 43 – 50
Color	Opaque	Clear	Clear
References	Dow Corning Inc.	(1)	This work

1. Zhu, S., et al., Ultrastretchable Fibers with Metallic Conductivity Using a Liquid Metal Alloy Core. Advanced Functional Materials, 2013. 23(18): p. 2308-2314.

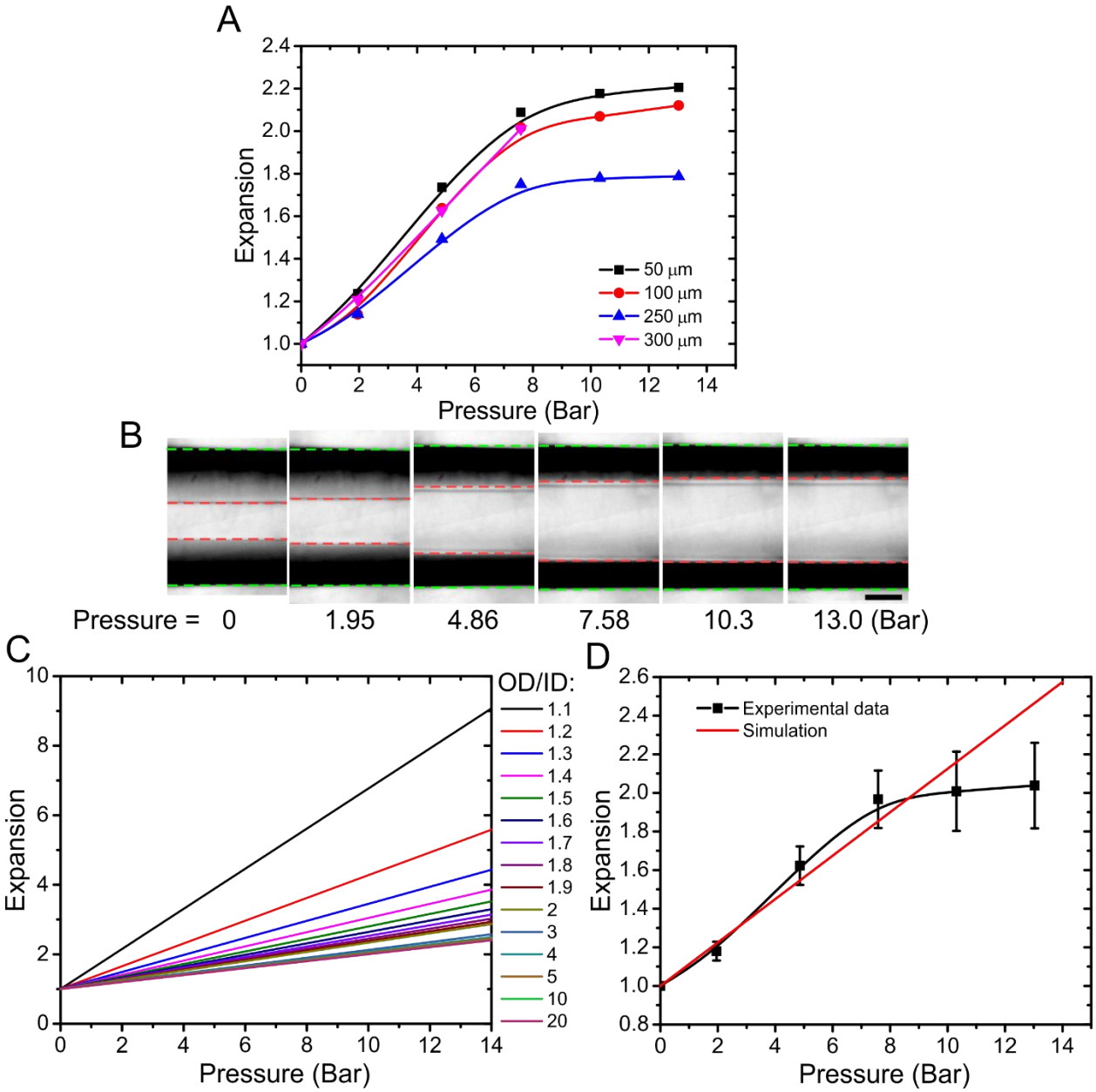

Fig. S6. (*A*) The normalized expansion of IDs of various microtubes as a function of intraluminal pressure. The IDs of the microtubes are listed in the lower right corner. The OD/ID ratio is one main factor that influences the expansion of the tubing. For all the microtubes, OD/ID = 3:1. (*B*) Optical images revealing the expansion of one PDMS microtube (ID = 50 μm and OD/ID = 3:1) as intraluminal pressure was increased. Red dash lines: inner wall; green dashlines: outer wall; scale bar: 50 μm. (*C*) Numerical analysis showing the linear expansion of perfect elastic tubes as a function of intraluminal pressure. (*D*) The experimental data for OD/ID = 3:1 is consistent with simulated expansion when pressure is smaller than 14 Bar.

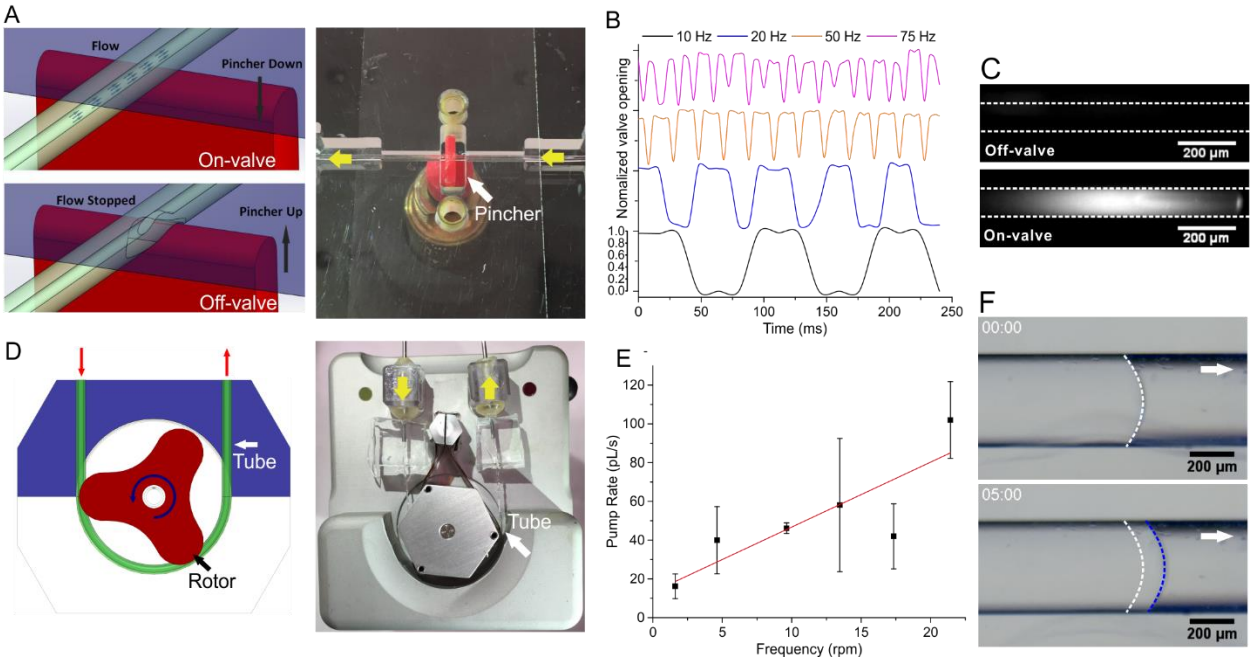

Fig. S7. Formation of microfluidic valve and pump with microtubes. (*A*) Schematic representation of an on-off valve. The valve is operated by periodically compressing a PDMS microtube with a mechanical pincer. Right, photo of the actual device. Yellow arrows indicate the microtube layout and the flow direction. White arrow indicates the position of the pincher. (*B*) The time response of opening and closing of a microtube (100 µm inner diameter) at different frequencies. The opening and closing of the microtube are measured by the intensity of the fluorescence inside the tube. (*C*) The normalized fluorescent intensity varying as a function of time is shown here. The abrupt increase and decrease in the fluorescent signal indicate a fast response of the microtube to the mechanical compression with minimum delay and the valve functions reasonably well up to 75 Hz, which is the limit of the solenoid. (*D*) Schematic representation of a peristaltic pump compressing a PDMS microtube (indicated by the white arrow) with ID = 100 µm. The rotor (the black arrow) occludes the flexible microtube and forces the fluid inside to be pumped through (the red arrows) as it turns (the blue arrow). Different pumping rates were achieved by rotating the rotor at various speeds. Right, photo of the actual device. Yellow arrows indicate flow direction. (*E*) Pumping rate of the peristaltic pump versus rotating speed. (*F*) Time lapse images showing the advancing fluid front in a time period of 5 minutes in the outlet of the peristaltic pump. White and blue dash lines show the advancement of the fluid front. White arrow indicates the flow direction.

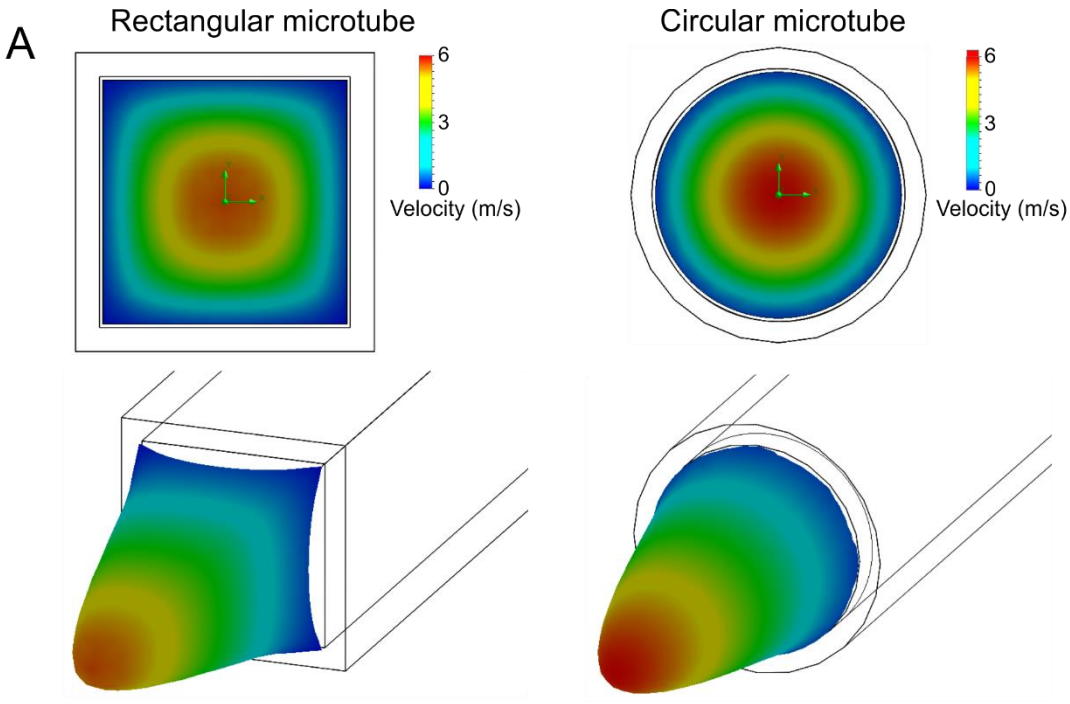
A
Rectangular microtube
Circular microtube
6
3
0
Velocity (m/s)
6
3
0
Velocity (m/s)

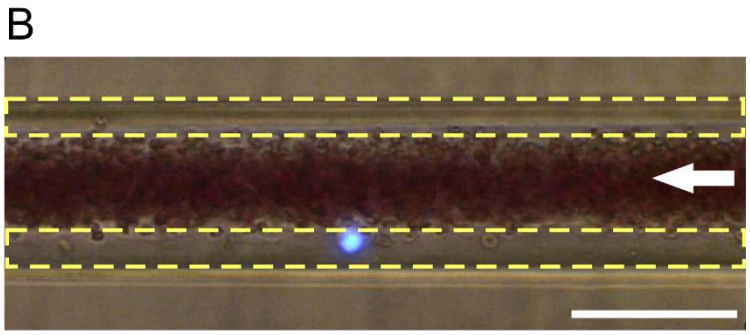
B

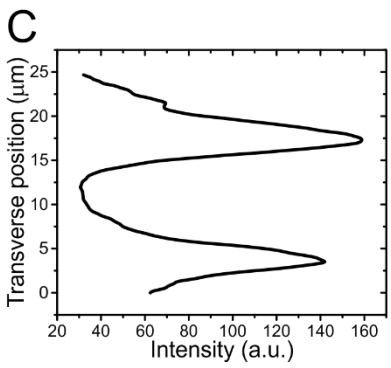
C
Transverse position (μm)
25
20
15
10
5
0
20
40
60
80
100
120
140
160
Intensity (a.u.)

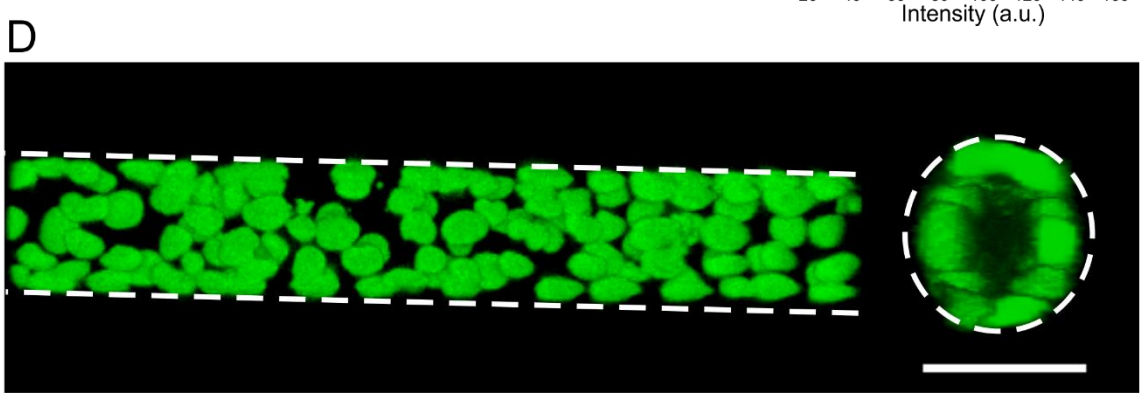
D

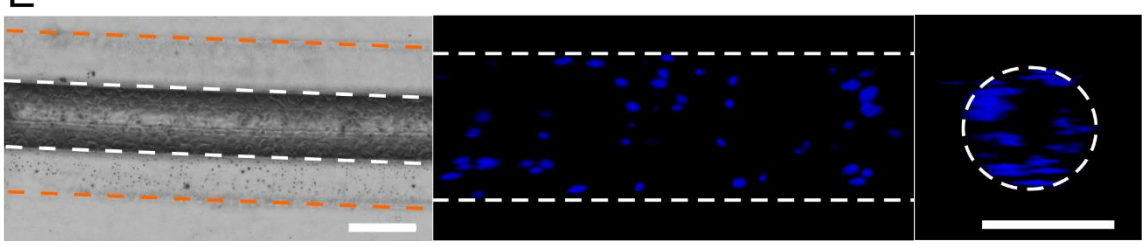
E

Fig. S8. Flow characteristics and cell functionalization inside circular microtubes. (*A*) Simulations of cross-sectional flow velocity profiles (2D profiles in upper panel and 3D profiles in lower panel, respectively) at outlets of a square microtube (left) and a circular microtube (right). The circular microtube (ID = 100 μm) and the square microtube have the same cross-sectional area. Other boundary conditions are: inlet/outlet pressure different is 1 Bar, and the lengths of the channels are 10 mm. (*B*) A typical optical image showing the margination effect of a HeLa cell in a circular microtube with ID = 25 μm. The white arrow indicates the flow direction and red blood cells (40% haematocrit in a whole blood sample) in the middle of the tube. The HeLa cells (stained blue due to DAPI staining) being positioned near to the cell-free plasma zone (as indicated by the yellow dash boxes) adjacent to the vessel wall is shown. Scale bar: 25 μm. (*C*) Fluorescent intensity profile, measured across the tubular channel in (*B*), demonstrates the HeLa cell distribution near the walls. (*D*) Fluorescent images of nuclei of epithelial cells (MDCK cells expressing H1-GFP) growing on the inner circumference (as indicated by the white dash lines) of a PDMS microtube (ID = 50 μm) for 24 hours, left: side view; right: cross-sectional view. Scale bars: 50 μm. (*E*) Bright field (left) and fluorescent images (DAPI; middle: side view and right: cross-sectional view) showing the growth of endothelial cells (HUVECs) on the inner wall (as indicated by the white dash lines) of a PDMS circular tube (ID = 100 μm). The orange dash lines indicate the outer surfaces of the tube. Scale bars: 100 μm.

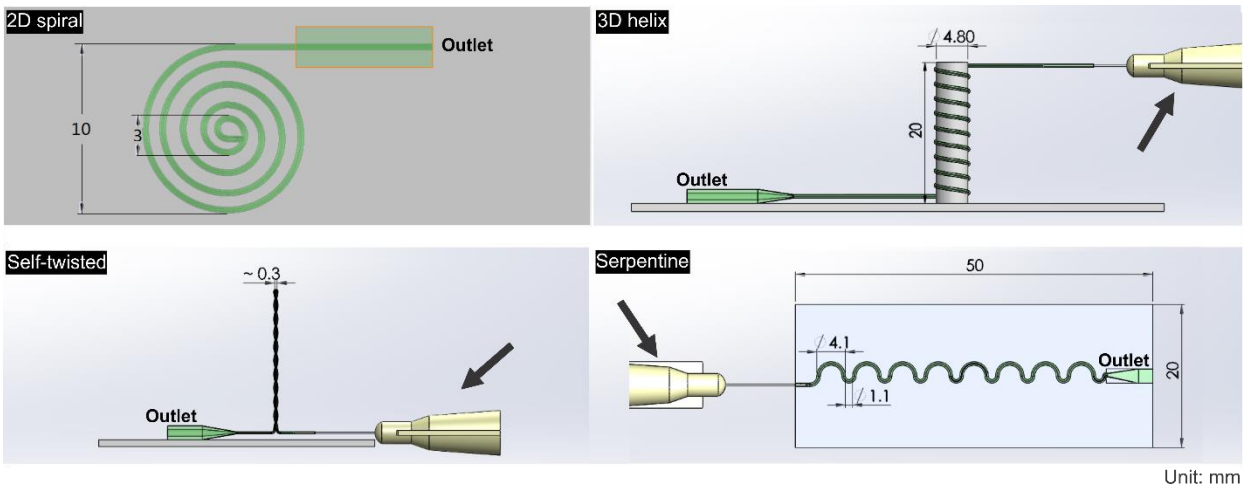

Fig. S9. Schematic drawings of the different microtube-formed chips for micro-bead (polystyrene, Φ = 10, 15, 20 and 25 μm) focusing and separation. The microtubes used for these designs have an ID = 100 μm and an OD = 300 μm.

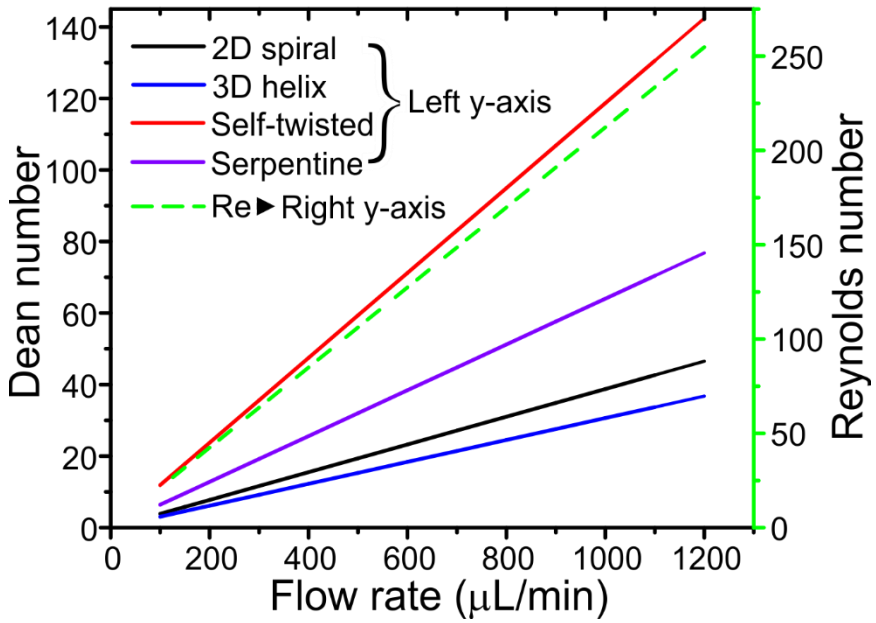

Fig. S10. The calculated D_e and Re as a function of the flow rate for each configuration.

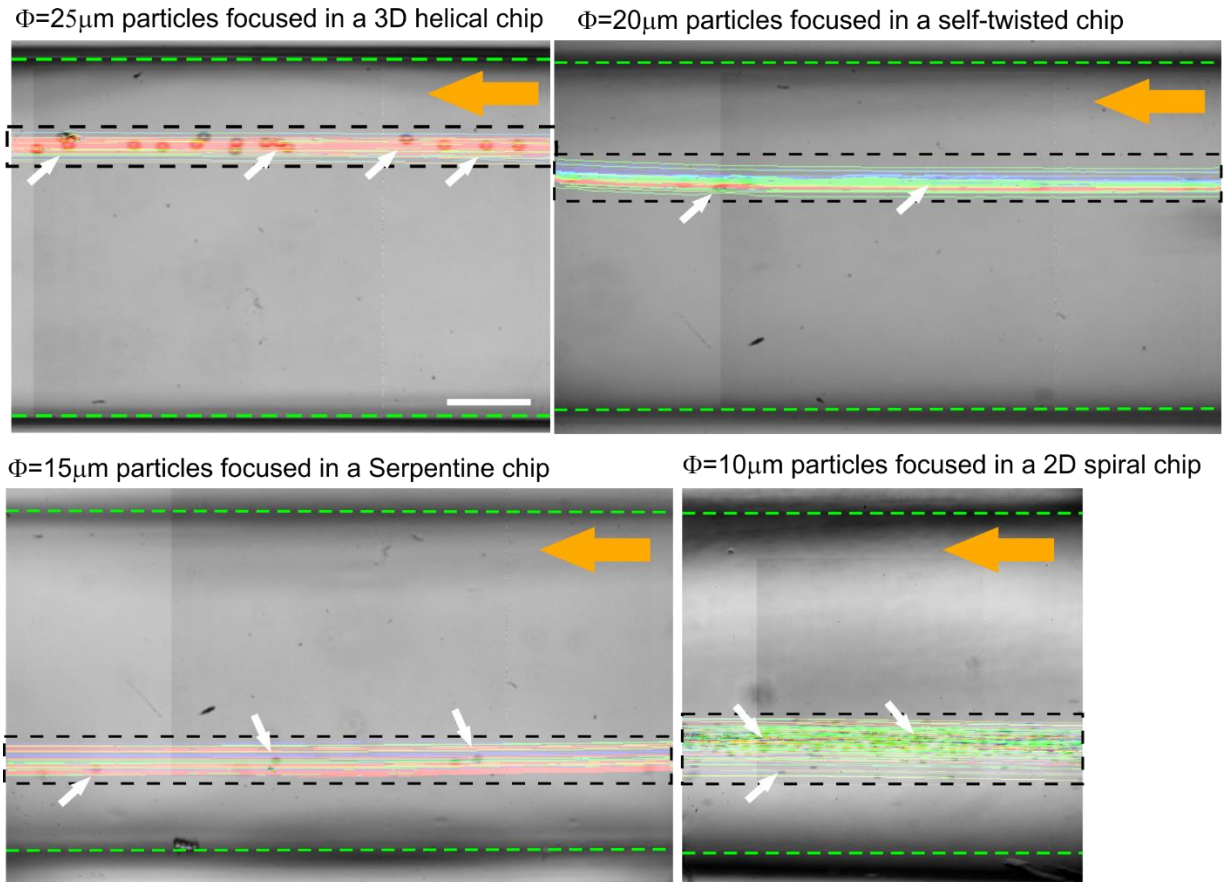

Fig. S11. Representative images showing focused microbeads (polystyrene, Φ = 25, 20, 15, and 10 μm) distribution at the outlets of chips of different configurations. The horizontal lines of different colours indicate tracking trajectories of the microparticles under flow. The width of the focused zones (indicated by the black dash boxes) is only ~10 to 20% the transverse dimension of the channels at the outlets. The orange arrows indicate the flow direction and the white arrows indicate the microparticles. Scale bar: 200 μm.

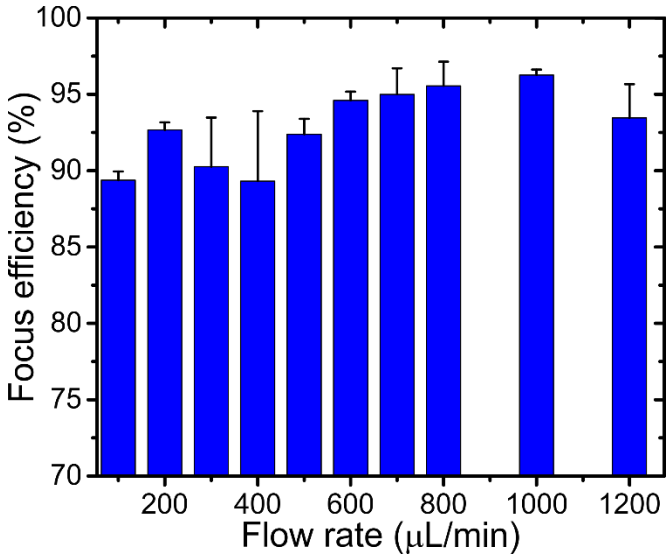

Fig. S12. Histogram of focus efficiency for microparticles (polystyrene, $\Phi = 25$ μm) in a 3D helical chip (Fig. S7) as a function of varying flow rates.

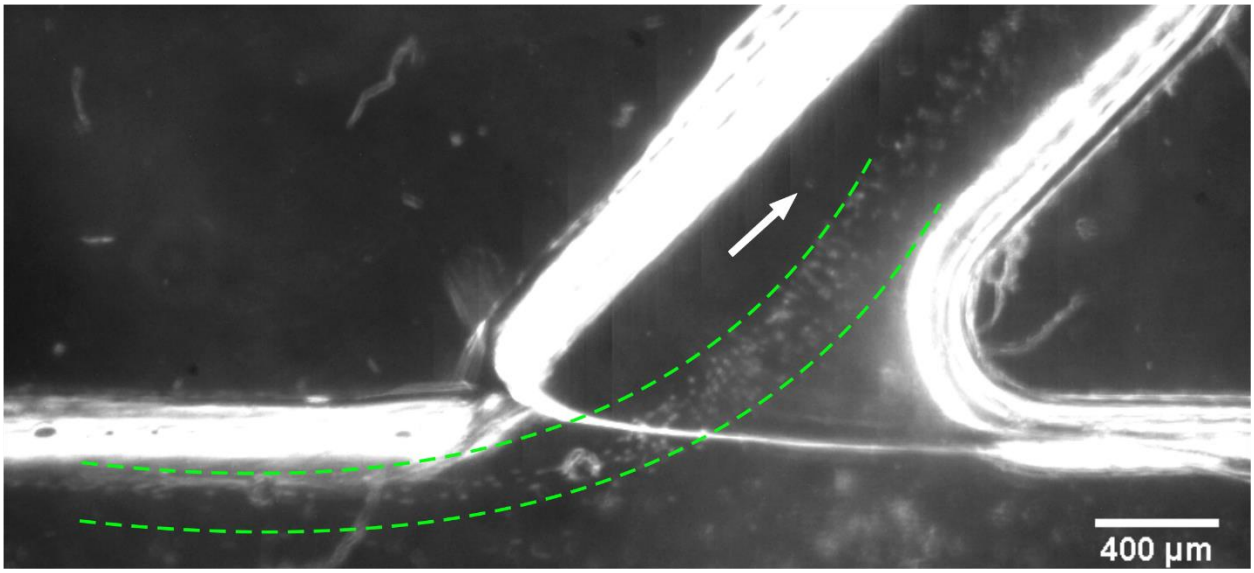

Fig. S13. MCF-10A cells (diameter ≈ 20 µm) focused to narrow streamlines and retrieved using 3D helical chip. The image showing the outlet of the device. White arrow indicates flow direction and focus zone is between green dash lines.

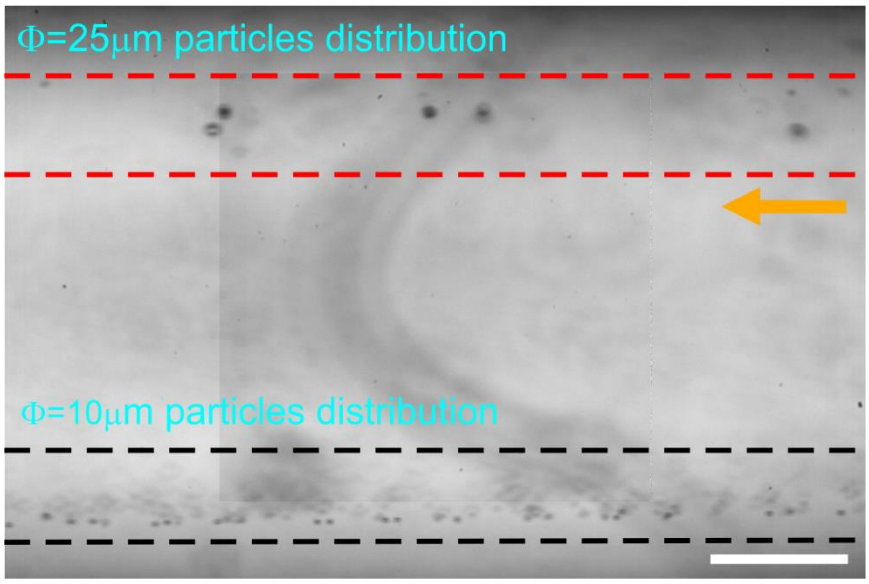

Fig. S14. Particles of 10 and 25 μm in diameter were focused into separate streamlines (between the black and red dash lines, respectively) in the outlet of a 3D helical chip. Scale bar: 150 μm.

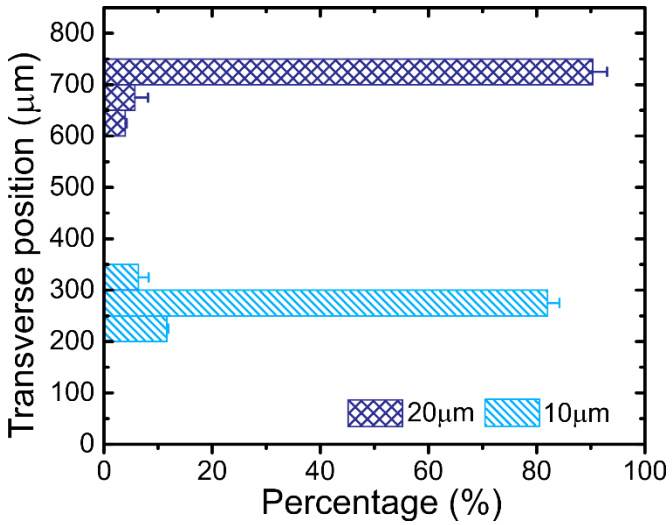

Fig. S15. Lateral position of polystyrene microparticles with diameters of 10 and 20 μm in the expanded outlet of a 3D helical chip.

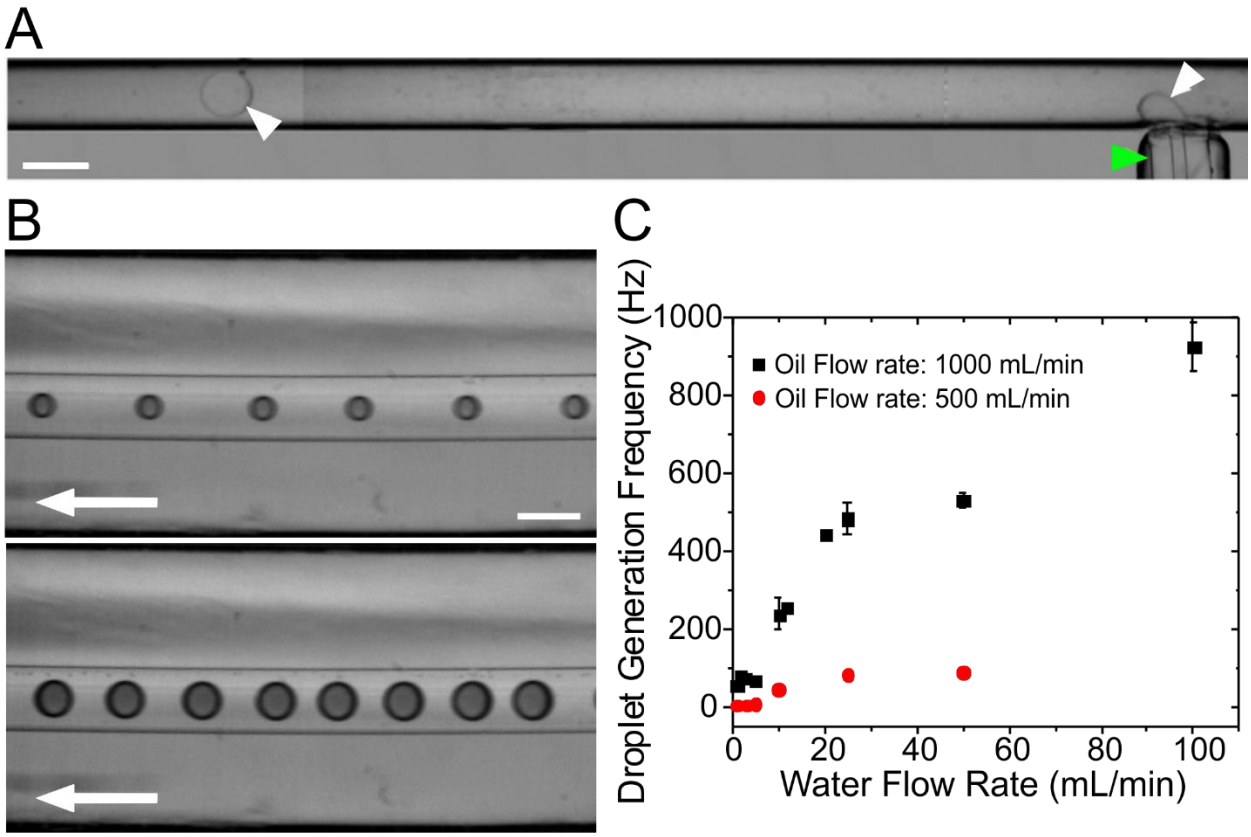

Fig. S16. Monodisperse water microdroplet generation in STmF chips. (*A*) A microtube (ID = 50 μm, green arrowhead) was inserted into a pre-made PDMS T-junction. Oil was flowing through the horizontal channel whereas water was flowing out of the microtube. This configuration enables generation of monodisperse microdroplets (here, water droplets indicated by the white arrowheads) in a high-throughput mode. Scale bar: 250 μm. (*B*) Optical images showing water droplets of a uniform diameter in a continuous oil flow (left image) and water droplets of changing diameters in an interrupted oil flow (lower image). The white arrows indicate the flow direction and scale bar: 250 μm. (*C*) Frequency of aqueous droplet generation as a function of the water flow rate for varied carrier phase flow rates of 1000 μl/min (black squares) and 500 μl/min (red circles).